inter.noise
21-24 AUGUST
SCOTTISH EVENT CAMPUS
GLASGOW 2022

AUDIO-FREQUENCY SURFACE WAVES OVER MULTIPLE WIDTH AND DEPTH GROOVES

by Steve Mellish[‡] *and* Shahram Taherzadeh *and* Keith Attenborough
(*Faculty of STEM, The Open University, UK*)

ABSTRACT

Previous studies of airborne surface waves have been carried out at audio-frequencies over periodically rough surfaces formed by lighting lattices and bricks and at ultrasonic frequencies over mm *scale compound gratings involving grooves of the same depth but different widths. In this paper, a modal model, which has been found to give comparable predictions to BEM while being much faster to run is used, together with BEM, to investigate audio-frequency sound propagation over grooves of varying widths and depths in the order of* cm*. Predictions of excess attenuation spectra, pressure contours and zeroes in the effective reflection coefficient over grooves with multiple widths and depths are used to indicate the nature of the surface waves which involve overlapping quarter wavelength resonances. Predictions are extended to multiple depth grooved surfaces without and with porous infills.*

1. Introduction

Tolstoy [1] suggested a clear distinction between an evanescent surface mode and a true surface wave. The former exists only due to the geometric and boundary conditions imposed at a surface under excitation by an incident source and will not necessarily self sustain once the incident source is removed. An example of this is the evanescent field at the edge of an optical element under total internal reflection. A true surface wave, although excited initially by an incident disturbance, may persist in the absence of an incident field due to resonant properties of the surface itself. This work suggests the extent to which any periodic disturbance near to the surface[†] may be sustained, is a function of the resonant behaviour of the surface, much akin to the resonant behaviour of tuned circuits in electronics, so the distinction between a surface mode and surface wave is blurred and a matter of degree.

In this paper we shall consider surface waves from a theoretical perspective using a modal model for rectangular grooves. Much attention has been given to rectangular gratings due to the ease with which they may be modelled, realised and their readiness to support surface waves.

2. A modal model for predicting the resonance contour of multiple grooved surfaces

A modal model was derived by Hessel *et al.* [2] to investigate blazing of simple rectangularly grooved gratings in the electromagnetic domain and subsequently applied to acoustics with the purpose of investigating surface waves by Kelders and Allard *et al.* [3, 4]. The authors recently extended the method to predict acoustic point-to-point propagation [5] and then expanded the system of equations to include multiple grooved structures of the form in Figure 1, with or without a porous layer at the base of each groove [6]. The focus of our current research is to continue the work of Kelders *et al.* using the modal model to predict surface wave (SW) behaviour, but with the application of

[‡] Corresponding author: steve@melectronics.co.uk

[†] Which may in fact be propagating or evanescent, just that energy in the former is radiated whereas the latter is constrained to the surface

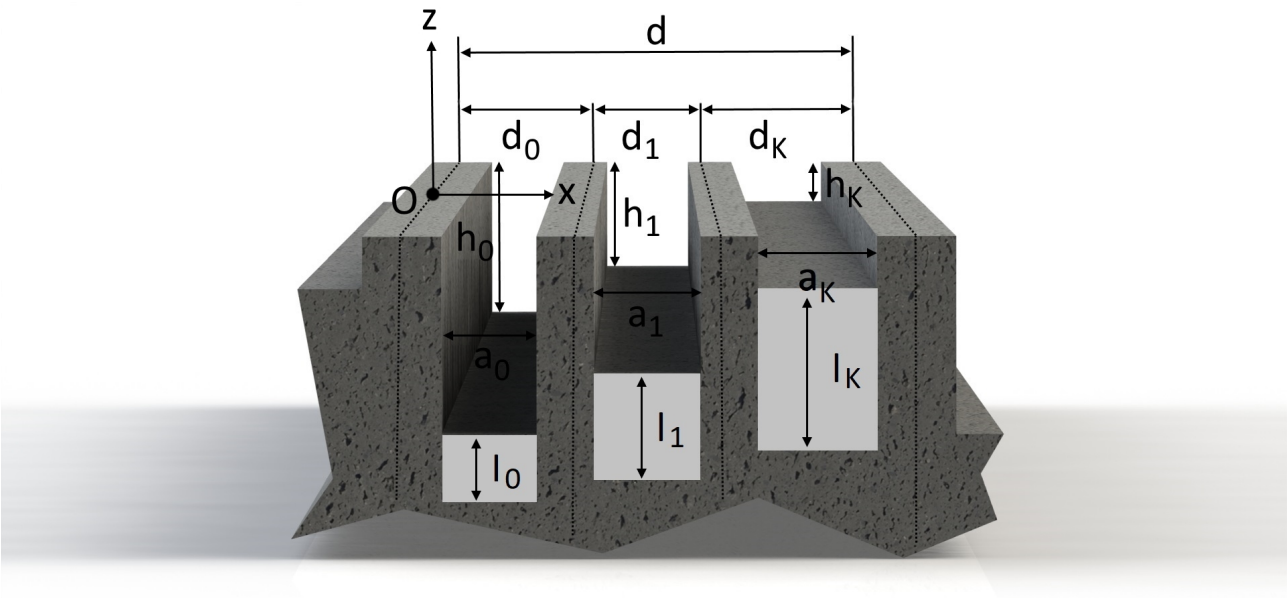

Figure 1: Multiple grooved periodic surface with porous layers.

our extensions to the model to admit more complex structures. The advances in computing power since the pioneering works also allow more involved simulations affording greater insight into the underlying physical processes involved.

Given the vertical axis is z, infinite spatial periodicity in the horizontal x-axis and invariance in y is assumed as is an $\exp(-i\omega t)$ time convention. A homogeneous plane wave is indcident upon the surface of the grating with angle of incidence (AOI) θ and propagation constant k, propagating in the x-z plane within an ideal inviscid medium. The modal model kernel is briefly described herein with full derivations to be found in [2–6].

The resulting 2d problem may be considered as a domain of two separate half spaces, a free field upper space for $z > 0$ and the lower groove space where $z < 0$. Continuity of pressure p and normal particle velocity v_z form the boundary conditions at the $z = 0$ surface. The acoustic field for the upper and lower space reduce respectively to infinite sets of m and n discrete modes, with complex amplitudes $\hat{V}_m$ (upper space quantities are denoted by hat) and V_n. The $\hat{V}_m$ and V_n sets are mutually related by an inner product relationship where $\hat{V}_0 = \hat{V}_0^i + \hat{V}_0^r$. The incident wave amplitude $\hat{V}_0^i$ is given as initial conditions of the problem along with the geometry of the grating. The modal impedances,

$$\hat{Z}_m = \frac{Z_c k}{\hat{k}_m^z}, \; \hat{Z}_m^i = -\hat{Z}_m^r = -\hat{Z}_0 \tag{1}$$

relate p to v_z for each free-space mode m, where Z_c is the characteristic impedance of the medium and the z-axis propagation constant $\hat{k}_m^z$ for each m is,

$$\hat{k}_m^z = \sqrt{k^2 - \left(k \sin\theta + \frac{2m\pi}{d}\right)^2} \tag{2}$$

and the x-axis projected propagation constant, $\hat{k}_m^x$, is given by the residual,

$$\hat{k}_m^x = \sqrt{k^2 - \hat{k}_m^{z\,2}}. \tag{3}$$

The propagation geometry of each m is defined by θ and the grating pitch d and has the mode function $\hat{e_m}$ upon $z = 0$,

$$\hat{e_m} = d^{-0.5} \exp\left(i\left[k\sin\theta + \frac{2m\pi}{d}\right]x\right). \tag{4}$$

Considering each groove to behave as an acoustically hard waveguide [7], the corresponding mode function $e_{q,n}$ across the aperture of each groove becomes,

$$\begin{aligned} e_{q,0} = \delta_e\sqrt{\frac{1}{a_q}},\ e_{q,n>0} =& \delta_e\sqrt{\frac{2}{a_q}}\cos\left(\left[\frac{n\pi}{a_q}\right]\left[x - \sum_{j<q} d_j + \frac{d_q - a_q}{2}\right]\right) \\ \delta_e =& \begin{bmatrix} 1 & x \geqslant \sum_{j<q} d_j + \frac{d_q - a_q}{2} \\ 1 & x \leqslant \sum_{j\leqslant q} d_j - \frac{d_q - a_q}{2} \\ 0 & else \end{bmatrix} j \in \mathbf{Z}^+ \end{aligned} \tag{5}$$

where index q denotes the q'th groove within each period from $q = 0$ to $q = K$ where $K + 1$ is the number of grooves per grating period d.

Truncating the infinite m and n sets and equating them at $z = 0$ results in the following system of equations, which may be solved numerically as a $K\ (N \times N)$ matrix of the form $\boldsymbol{A} * \boldsymbol{V_n} = \boldsymbol{B}$,

$$\begin{aligned} \sum_{q\dagger}\sum_{n\dagger} V_{q\dagger,n\dagger}\left(\sum_m\left[\hat{Z_m}\langle e_{q\dagger,n\dagger}, *\hat{e}_m\rangle\langle e_{q,n}, \hat{e}_m\rangle\right] - \delta_{q,n}^{q\dagger,n\dagger} Z_{q,n}\right) =& -2\hat{Z_0^i}\hat{V_0^i}\langle e_{q,n}, \hat{e}_0\rangle \\ \delta_{q,n}^{q\dagger,n\dagger} =& \begin{bmatrix} 1 & a = a\dagger, q = q\dagger \\ 0 & else \end{bmatrix}. \end{aligned} \tag{6}$$

The modal impedance at the mouth of each groove, $Z_{q,n}$, incorporating a porous layer element to the bottom of each groove is given by,

$$Z_{q,n} = \frac{Z_c k}{k_{q,n}}\frac{(-1 + \gamma\exp(ik_{q,n}2h_q))}{1 + \gamma\exp(ik_{q,n}2h_q)}, \text{ where } \gamma = -\frac{1 - (1/Z_L(q,n))}{1 + (1/Z_L(q,n))}. \tag{7}$$

Kelders *et al.* [3] realised that local minima in $\det \boldsymbol{A}$, relate to inherent resonances of the grating itself in the zeroth-mode x-axis wave function $\hat{k_0^x}$ at a particular frequency. Taking,

$$\nabla \cdot (\nabla \det \boldsymbol{A}) \tag{8}$$

and sweeping as a function of frequency and $\hat{k_0^x}$, provides a resonant response where local poles in the response represent incidences of resonance which are properties of the grating structure itself. This along with the propagation characteristics of each mode in the system, give useful insight into the physical processes which may not be apparent using other numerical techniques such as FEM or BEM.

3. Resonant characteristics of variable depth grooves

It has been shown [8, 9] that under certain conditions, surface wave characteristics or Excess-Attenuation (EA) maxima/minima may be predicted by considering rudimentary phenomenon such as $\frac{1}{4}$-Wavelength ($\frac{1}{4}\lambda$) resonance or phase gradient $\frac{\partial\phi}{\partial x}$ [10]. However, the system is complicated and not fully explained by any one effect, hence the need for complex numerical models to provide generic modelling. To explore the resonant characteristics of the rectangular grating a simple 2-grooved

structure with and without porous infill is considered initially. The depth of each groove has been chosen such that the idealised (no end correction) $\frac{1}{4}\lambda$ resonances lie at $1\,\mathrm{kHz}$ and $1.5\,\mathrm{kHz}$ respectively. The remaining geometry of the problem has been chosen arbitrarily to show responses of interest in the $1\,\mathrm{kHz}$ region as it is a significant nuisance band of road traffic noise [11]. Figure 2 shows the EA spectra for such a surface as predicted by the point-to-point propagation modal model [6] both with air-filled grooves and grooves fully filled with a porous medium (flow resistivity $\approx 869\,\mathrm{Pasm}^{-2}$, porosity 0.5), extending horizontally between the source and receiver with source and receiver heights of $0.03\,\mathrm{m}$, separated by $2\,\mathrm{m}$.

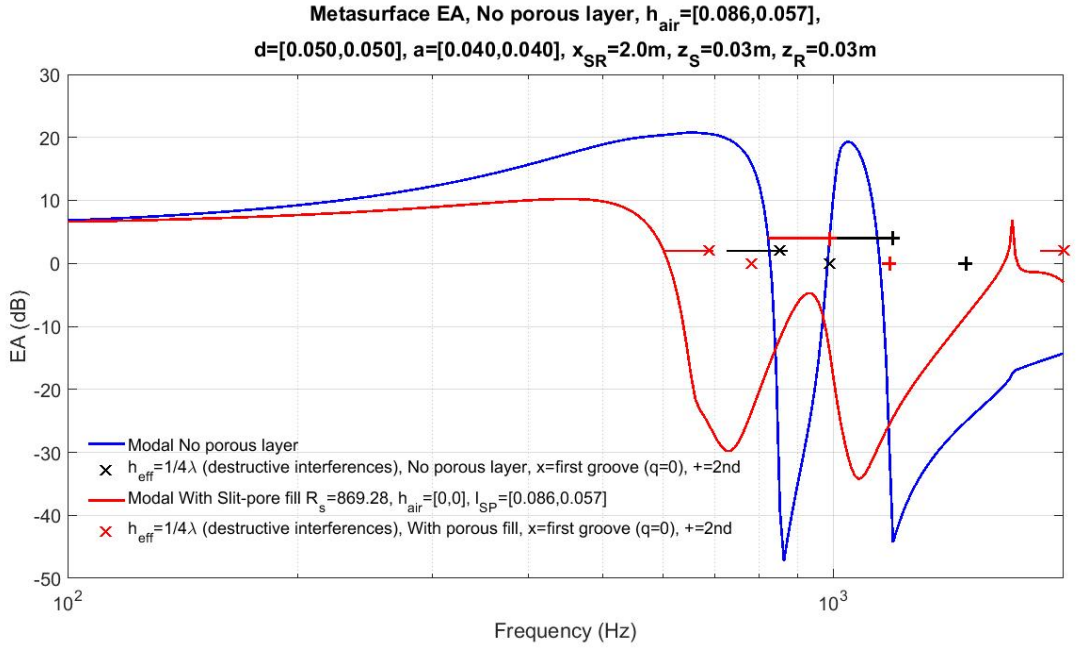

Figure 2: EA spectra for a 2-groove grating with geometry $d_0 = d_1 = 0.05\,\mathrm{m}$, $a_0 = a_1 = 0.04\,\mathrm{m}$ and $h_0 = 0.086\,\mathrm{m}, h_1 = 0.057\,\mathrm{m}$.

For each groove, the markers represent theoretical $\frac{1}{4}\lambda$ resonance frequencies and the horizontal line bars indicate the frequency band with an end correction applied in the range $0.31a_q$ to $\frac{\pi}{4}a_q$ [12]. Their location is consistent with the general expectation that at such frequencies the pressure field will tend to cancel near to the surface due to the $\approx \pi$ phase shift introduced by traversing the groove causing destructive interference with the incident mode.

Figure 3 shows the corresponding resonant contour plot of the 2-groove grating both with and without a porous infill, plotted against $\sin\theta$, where θ is the angle-of-incidence of the zeroth m-mode, which in the case of Figure 3 is imaginary and the entire domain of the plot represents evanescent surface modes. For the air filled case, the predicted SW resonant peaks (indicated by local maxima) agree in frequency with the EA response in Figure 2 at around $770\,\mathrm{Hz}$ and $1040\,\mathrm{Hz}$. From both the EA plot of Figure 2 and SW contour plot of Figure 3, it is evident that the addition of the porous layer attenuates any resonances as would be expected by adding loss to the system. Comparing these results with the time-independent pressure field BEM simulations of Figure 4, show consistency with the EA and SW contour results obtained from the modal model. Significant field enhancement is observed near to the surface at the predicted resonant frequenies of $770\,\mathrm{Hz}$ and $1040\,\mathrm{Hz}$ due to resonance of the

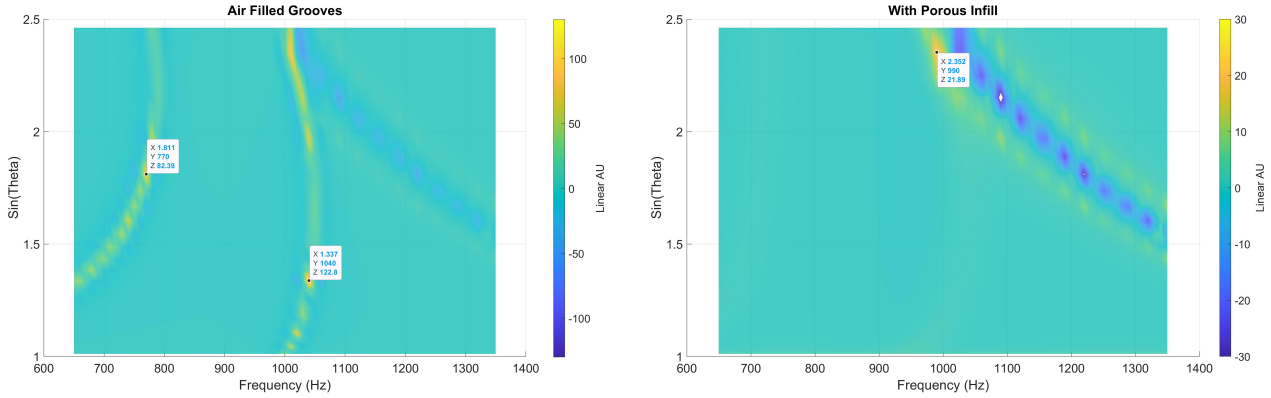

Figure 3: 2-groove SW resonant contour plot with a) Air filled grooves and b) Porous layer infill.

grating, induced by the incident mode. Strong attenuation occurs close to the surface around the $\frac{1}{4}\lambda$ resonance frequencies of 860 Hz and 1200 Hz.

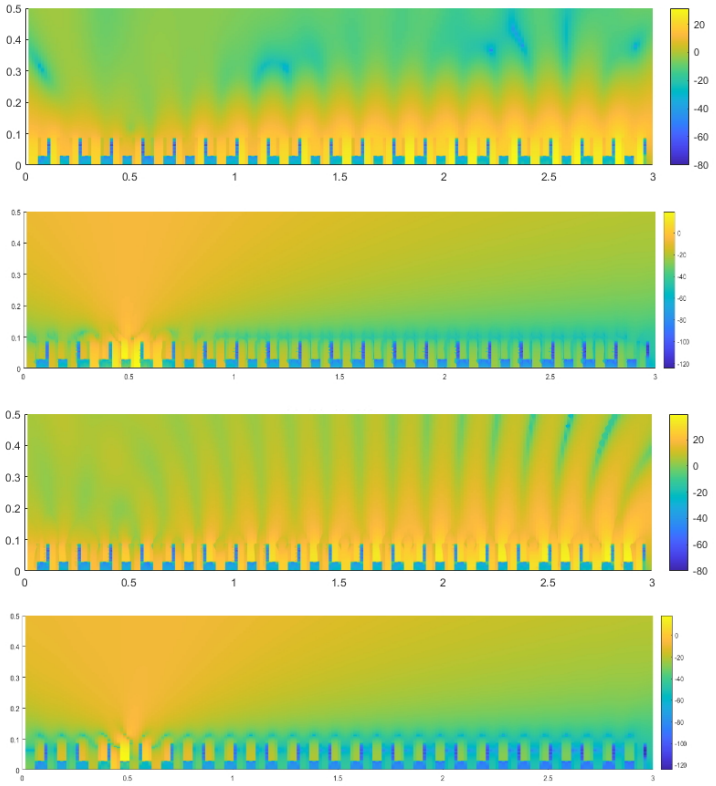

Figure 4: BEM simulation of the pressure field over air filled 2-groove surface with source and receiver heights of 0.03 m separated by 2 m (source @$x = 0.5$) at a) 770 Hz (top), b) 860 Hz, c) 1040 Hz and d) 1200 Hz (bottom).

4. Variable width grooves

Beadle *et al.* [13] studied a variable groove width geometry using both FEM and experimental methods. We shall apply the modal method to the same geometry to compare the results while gaining

insight into the features of variable width grooves. Figure 5 shows the resulting resonant contour for the first two Brillouin zones (BZ) in the fundamental projected x-axis wavenumber k_0^x normalised to the effective wavenumber of the grating period k_g.

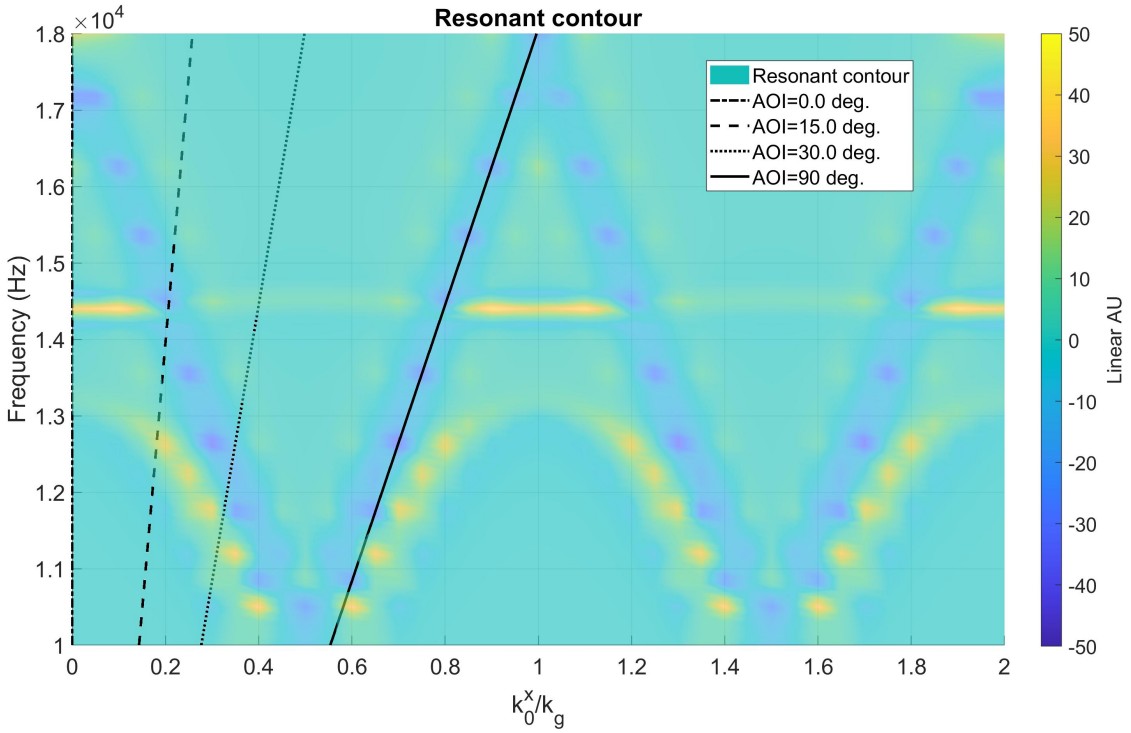

Figure 5: Resonance plot for Beadle variable width grating where $d_0 = d_2 = 0.006\,\mathrm{m}$, $d_1 = 0.007\,\mathrm{m}$, $a_0 = a_2 = 0.001\,\mathrm{m}$, $a_1 = 0.002\,\mathrm{m}$, $h_0 = h_1 = h_2 = 0.005\,\mathrm{m}$.

The hemispherical fundamental resonant response is due to interaction between adjacent grooves which occurs in various phase/anti-phase combinations depending upon the geometry and resulting degrees-of-freedom, whereas the flat resonant line at $\approx 14.25\,\mathrm{kHz}$ is related to the $\frac{1}{4}\lambda$ frequency of the groove depth h with a corresponding end correction.

The trio of grooves per period exhibit odd symmetry about $k_0^x/k_g = 0.5$ whereas the two groove structure of the previous section would show even symmetry were it plotted in the same format. As expected, symmetry is observed at the BZ boundary. Beadle *et al.* (their Figure 2) predicted absorption minima at $\approx 13\,\mathrm{kHz}$, $\approx 12.5\,\mathrm{kHz}$ and $\approx 11.25\,\mathrm{kHz}$ for plane wave angles of incidence of $0°$, $15°$ and $30°$ respectively. For qualitative comparison the k_0^x/k_g lines are plotted for the three AOI's, each of which intersect an area of resonance at each respective absorption frequency. This indicates that incident energy is being re-directed away from the specularly reflected mode as confirmed by the blazing clearly seen to coincide with each absorpton frequency in the modal energy distribution plots of Figure 6. In this set of figures the three plots in the left column show the magnitude of the diffraction modes in the range $m = -2$ to $m = 1$ with respect to each frequency for each AOI, with the cut-off frequency relating to each mode plotted as a vertical dotted cursor if within the plotted frequency bandwidth. The text boxes "Min@..", "Coinc@.." and "Max@.." show the x-axis wavenumber k_x, k_x/k_g and frequency values at the minimum magnitude of the specularly reflected mode component of $m = 0$, at the maximum magnitude of a higher order diffraction mode $|m| > 0$ and the properties of the maximally diffracted mode at the minima frequency of $m = 0$

respectively. In the right hand column are graphical representations of real and imaginary parts of the wave functions of the incident and largest magnitude diffracted mode, at each blazing frequency, with the grating structure shown in red, whose period is delimited by the black vertical cursors.

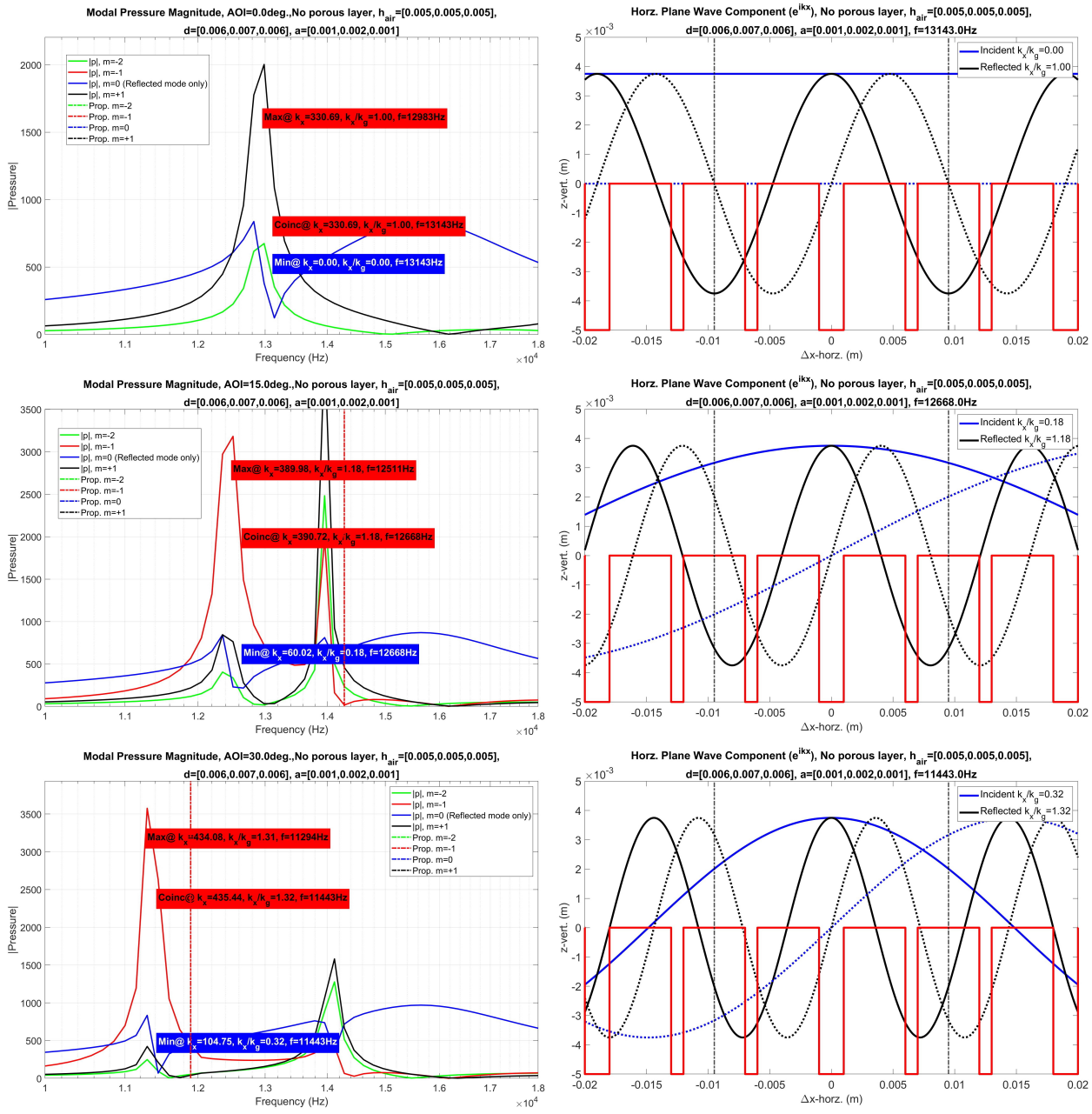

Figure 6: Modal magnitude distribution (left column) and projected phase (right column, $\Re$ solid trace and $\Im$ dotted trace) of incident and reflected modes with an AOI of a) 0°, b) 15°and c) 30°.

Due to the symmetry of the problem, at perpendicular incidence both $m = -1$ and $m = 1$ are equally excited at the absorption frequencies measured by Beadle *et al.* , whereas at $15°$ and $30°$ energy is directed primarily into $m = -1$.

The close proximity of a minimum in $m = 0$ and a maximum in a higher order mode signifies blazing, which manifests in the Figure 2 results of Beadle *et al.* as absorption minima. At each

absorption/blazing frequency, incident energy in the zeroth mode $m = 0$ is redistributed into a higher order diffraction mode $|m| > 0$ in the next BZ with x-axis wavenumber $k_0^x + k_g$.

5. Conclusions

The resonant properties of a multiple rectangular grooved grating may be extensively profiled using a computationally efficient modal technique suggested by Kelders *et al.* The method has been expanded to permit multiple grooved surfaces as well as a porous infill and the results have been shown consistent with BEM and FEM methods but with faster solution times, as well as with experimental data. Moreover the modal method affords useful insight into the physical processes involved.

6. References

[1] I. Tolstoy, Smoothed boundary conditions, coherent low-frequency scatter, and boundary modes, *J. Acoust. Soc. Am.* **75** (1984) 1–22.

[2] A. Hessel, J. Schmoys and D.Y. Tseng, Bragg-angle blazing of diffraction gratings, *Journal of the optical society of America* **65** (1975) 380–384.

[3] L. Kelders, J.F. Allard and W. Lauriks, Ultrasonic surface waves above rectangular-groove gratings, *J. Acoust. Soc. Am.* **103** (1998) 2730–2733.

[4] J.F. Allard, L. Kelders and W. Lauriks, Ultrasonic surface waves above a doubly periodic grating. *J. Acoust. Soc. Am.*, **105** (1999) 2528–2531.

[5] S. Mellish, S. Taherzadeh and K. Attenborough, Approximate impedance models for point-to-point sound propagation over acoustically-hard ground containing rectangular grooves, *J. Acoust. Soc. Am.*, **147** (2020) 74–84.

[6] S. Mellish, S. Taherzadeh and K. Attenborough, Use of a modal model in predicting propagation from a point source over grooved ground, *Q. Jl Mech. Appl. Math*, **Vol. 73. Issue. 4** (2021) 367–382.

[7] D.T. Blackstock, *Fundamentals of physical acoustics* (Wiley-Interscience, New York, USA, 2000).

[8] I. Bashir, S. Taherzadeh and K. Attenborough, Diffraction-assisted rough ground effect: models and data, *J. Acoust. Soc. Am.* **133** (2013) 1281–1292.

[9] D. Berry, S. Taherzadeh and K. Attenborough, Acoustic surface wave generation over rigid cylinder arrays on a rigid plane, *J. Acoust. Soc. Am.* **146(4)** (2019) 2137–2144.

[10] S. Larouche and D.R. Smith Reconciliation of generalized refraction with diffraction theory, *Optics Letters* **Vol. 37. No. 12** (2012) 2391–2393.

[11] K. Attenborough, S. Taherzadeh, T. Hill, I. Bashir, J. Forssen and M. Hornikx, The acoustical performance of parallel wall systems, *HOSANNA* **WP4** (2012) 1–69.

[12] A.D. Pierce, *Acoustics: An Introduction to Its Physical Principles and Applications* (Springer International Publishing, New York, USA, 2019).

[13] J.G. Beadle, T. Starkey, J.A. Dockrey, J.R. Sambles and A.P. Hibbins The acoustic phase resonances and surface waves supported by a compound rigid grating, *Sci. Rep.* **8:10701** (2018) 1–7.